Long-range interactions in a quantum gas mediated by diffracted light

G. R. M. Robb, J. G. M. Walker, G.-L. Oppo, and T. A. Ackemann

SUPA and Department of Physics, University of Strathclyde, Glasgow G4 0NG, Scotland, United Kingdom

A Bose-Einstein condensate (BEC) interacting with an optical field via a feedback mirror can be a realization of the quantum Hamiltonian Mean Field (HMF) model, a paradigmatic model of long-range interactions in quantum systems. We demonstrate that the self-structuring instability displayed by an initially uniform BEC can evolve as predicted by the quantum HMF model, displaying quasiperiodic "chevron" dynamics for strong driving. For weakly driven self-structuring, the BEC and optical field behave as a two-state quantum system, regularly oscillating between a spatially uniform state and a spatially periodic state. It also predicts the width of stable optomechanical droplets and the dependence of droplet width on optical pump intensity. The results presented suggest that optical diffraction-mediated interactions between atoms in a BEC may be a route to experimental realization of quantum HMF dynamics and a useful analog for studying quantum systems involving long-range interactions.

Systems involving long-range interactions, such as those occurring in gravitational physics or plasma physics, display several unusual behaviours, e.g., extremely slow relaxation and existence of quasisteady states [1]. Recently, there has been significant interest in quantum systems involving long range interactions, e.g., ion chains, Rydberg gases, and cold atomic gases enclosed in optical cavities [2].

The Hamiltonian Mean Field (HMF) model [1] was introduced as a generic classical model of long-range interacting systems, e.g., self-gravitating systems [3]. It involves N particles on a ring which experience a pairwise cosine interaction. It also arises as a model of a system of X-Y rotors coupled with infinite range. Extension of the HMF model to describe quantum systems was first carried out by Chavanis [4,5] and the dynamics of this quantum HMF model was investigated more recently by Plestid and O'Dell [6,7], who demonstrated that the model exhibited violent relaxation of an initially homogeneous state to a structured state and possessed bright soliton solutions.

Cold atomic gases enclosed in cavities exhibit phenomena demonstrating universal behaviors common to many different physical systems, e.g., the behavior of a cold, thermal gas in a cavity undergoing viscous momentum damping induced by optical molasses beams is related to the Kuramoto model [8,9] which describes synchronization of globally coupled phase oscillators. It has been shown [10,11] that in the absence of momentum damping, a thermal gas in a cavity can exhibit dynamics similar to that of the classical HMF model. In the case of a quantum degenerate gas, e.g., a Bose-Einstein condensate (BEC), its dynamical behavior in a cavity has been

mapped onto the Dicke model describing coupled spins and superradiance [12], but to date no experimental realization of the quantum HMF model has been described or proposed.

Here we investigate a system consisting of a BEC interacting with an optical field via single mirror feedback (SMF) as shown schematically in Fig. 1. In this BEC-SMF system, coupling between atoms arises due to diffraction, involves many transverse modes, and optical forces are directed perpendicular to the propagation direction of the optical fields. This is significantly different from cavity systems (such as, e.g., Refs. [9,12]), where the dominant coupling between atoms arises from interference between a pump field and cavity modes. We show that under certain conditions, the equations describing the dynamics of the BEC and the optical fields can be mapped onto the quantum HMF model [4–6]. Using this connection, we then investigate dynamical instabilities of initially homogeneous distributions of BEC density and optical intensity and also the existence of spatially localized states reminiscent of quantum droplets observed in dipolar BECs [13,14]. The model we use to describe the BEC-SMF system was originally studied in Ref. [15] as an extension of that used to study self-structuring of a classical, thermal gas, observed experimentally in Ref. [16], with the thermal gas replaced with a BEC. We consider a BEC with negligible atomic collisions and describe the evolution of the BEC wavefunction $\Psi(x, t)$ with the Schrödinger equation

$$i\hbar \frac{\partial \Psi(x, t)}{\partial t} = -\frac{\hbar^2}{2m} \frac{\partial^2 \Psi(x, t)}{\partial x^2} + \frac{\hbar\delta}{2} s(x, t)\Psi(x, t), \quad (1)$$

where m is the atomic mass, $\delta = \omega - \omega_a$ is detuning, $s(x, t) = |F|^2 + |B(x, t)|^2$ is the atomic saturation parameter due to the forward and backward optical fields where $|F|^2 = \frac{I_F}{I_{sat}\Delta^2}$, $|B|^2 = \frac{I_B}{I_{sat}\Delta^2}$, and I_F, I_B are the intensities of the forward (F) and backward (B) fields respectively. I_{sat} is the saturation intensity on resonance, $\Delta = \frac{2\delta}{\Gamma}$, and Γ is the decay rate of

the atomic transition. It has been assumed that $|\Delta| \gg 1$ and that consequently $s \ll 1$ so that the atoms remain in their ground state. In addition, longitudinal grating effects due to interference between the counterpropagating optical fields are neglected.

In order to describe the optical field in the gas we assume that the gas is sufficiently thin that diffraction can be neglected, so that the forward field transmitted through the cloud is

$$F_{tr} = \sqrt{p_0} \exp\left(-i\chi_0 n(x, t)\right), \qquad (2)$$

where $p_0 = |F(z = 0)|^2$ is the scaled pump intensity, $\chi_0 = \frac{b_0}{2\Delta}$ is the susceptibility of the BEC, b_0 is the optical thickness of the BEC at resonance, and $n(x, t) = |\Psi(x, t)|^2$ is the local BEC density, which for a BEC of uniform density is $n(x, t) = 1$.

The backward field B at the BEC completes the feedback loop. As the field propagates a distance $2d$ from the BEC to the mirror and back, optical diffraction plays a critical role by converting phase modulations to amplitude modulations and consequently optical dipole forces. The relation between the Fourier components of the forward and backward fields at the BEC is

$$B(q) = \sqrt{R}F_{tr}(q)e^{i\frac{q^2 d}{k_0}}, \qquad (3)$$

where R is the mirror reflectivity, q is the transverse wavenumber, and $k_0 = \frac{2\pi}{\lambda_0}$. It was shown in Ref. [15] that this system exhibits a self-structuring instability where the optical fields and BEC density develop modulations with a spatial period of $\Lambda_c = \frac{2\pi}{q_c}$, where the critical wavenumber q_c is

$$q_c = \sqrt{\frac{\pi}{2}\frac{k_0}{d}}. \qquad (4)$$

The reason for this instability is that BEC density modulations (which produce refractive index modulations), with spatial frequency q_c, produce phase modulations in F_{tr} which are in turn converted into intensity modulations of B [see Eq. (3)]. These intensity modulations produce dipole forces which reinforce the density modulations, resulting in positive feedback and instability of the initial, homogeneous state. A condition of this instability is that the pump intensity exceeds a threshold value p_{th} [15], which for $q = q_c$ can be written as

$$p_{th} = \frac{2\omega_r}{b_0 R \Gamma}, \qquad (5)$$

where $\omega_r = \frac{\hbar q_c^2}{2m}$.

The optomechanical self-structuring exhibited by the BEC-SMF model of Eqs. (1)–(3) derived in Ref. [15] can be reduced to that of the quantum HMF model, originally proposed in Refs. [4,5] and revisited in Refs. [6,7]. We express the optical intensity $s(x, t)$ in terms of n (density) using Eq. (2). Assuming $\chi_0 n \ll 1$ as in Ref. [17], then $F_{tr} \approx \sqrt{p_0}(1 + i\chi_0 n(x, t))$. It is assumed that the BEC density and (backward) optical field consist of a spatially uniform component and a spatial modulation with spatial frequency q_c, so

$$B(q_c) = \sqrt{R}F_{tr}(q_c)e^{i\frac{q_c^2 d}{k_0}} = i\sqrt{R}F_{tr}(q_c), \qquad (6)$$

i.e., phase modulation of F_{tr} becomes amplitude modulation of B. Expressing

$$F_{tr}(x, t) = F_{tr}^{(0)} + F_{tr}^{(q_c)}e^{iq_c x} + F_{tr}^{(-q_c)}e^{-iq_c x},$$

$$n(x, t) = 1 + n^{(q_c)}e^{iq_c x} + n^{(q_c)*}e^{-iq_c x},$$

then substitution of the above into Eq. (2) shows that

$$\left.\begin{array}{c} F_{tr}^{(0)} = \sqrt{p_0}(1 + i\chi_0) \approx \sqrt{p_0} \\ F_{tr}^{(q_c)} = i\sqrt{p_0}\chi_0 n^{(q_c)} \\ F_{tr}^{(-q_c)} = i\sqrt{p_0}\chi_0 n^{(q_c)*} \end{array}\right\}. \qquad (7)$$

Using a similar expansion of $B(x, t)$ and then Eqs. (6), (7) produces

$$B = \sqrt{Rp_0} - \sqrt{Rp_0}\chi_0 n^{(q_c)}e^{iq_c x} - \sqrt{Rp_0}\chi_0 n^{(q_c)*}e^{-iq_c x}.$$

Writing $n^{(q_c)} = |n^{(q_c)}|e^{-i\phi}$, then

$$B = \sqrt{Rp_0} - 2\sqrt{Rp_0}\chi_0|n^{(q_c)}|\cos(q_c x - \phi), \qquad (8)$$

which allows us the optical field intensities in Eq. (1) to be written in terms of the BEC density

$$s(x, t) \approx p_0 + Rp_0 - 4Rp_0\chi_0|n^{(q_c)}|\cos(q_c x - \phi). \qquad (9)$$

Note that if the assumption $\chi_0 n \ll 1$ was relaxed, additional terms with spatial frequency $2q_c$ would also be present. As $n^{(q_c)}$ is described by $n^{(q_c)} = \frac{1}{L}\int_0^L |\Psi(x, t)|^2 e^{-iq_c x}\,dx$, where L is the BEC length then

$$|n^{(q_c)}|\cos(q_c x - \phi) = \frac{1}{2\pi}\int_0^{2\pi} |\Psi(\theta', t)|^2 \cos(\theta - \theta')\,d\theta',$$

where $\theta = q_c x$ and it has been assumed that Ψ is spatially periodic with period Λ_c. Consequently, Eq. (9) can be written as

$$s(x, t) = p_0 + Rp_0 - 4Rp_0\chi_0\Phi(\theta, t), \qquad (10)$$

where the nonlocal potential $\Phi(\theta, t)$ is $\Phi(\theta, t) = \frac{1}{2\pi}\int_0^{2\pi} |\Psi(\theta', t)|^2 \cos(\theta - \theta')\,d\theta'$. The constant term in Eq. (10) results in a constant potential energy contribution to Eq. (1), which can be eliminated by the transformation Ψ via $\Psi = \Psi'\exp(-i\frac{(1+R)p_0\delta}{2}t)$, so that the Schrödinger equation from Eq. (1) becomes a Gross-Pitaevskii equation (GPE) analog

$$i\frac{\partial\Psi'}{\partial t} = -\omega_r\frac{\partial^2\Psi'}{\partial\theta^2} - \epsilon\Phi(\theta, t)\Psi', \qquad (11)$$

where $\epsilon = 2\delta Rp_0\chi_0 = \frac{Rp_0 b_0\Gamma}{2} = \frac{p_0}{p_{th}}\omega_r$. Equation (11) has the same effective GPE-like form as that of the quantum HMF model [4,6]. Note that $\epsilon > 0$ always, which corresponds to the case of the ferromagnetic quantum HMF model. The order parameter or magnetization M is essentially the Fourier component of the BEC density with spatial frequency q_c [5,6]:

$$M = \left|\frac{1}{2\pi}\int_0^{2\pi} |\Psi|^2 e^{i\theta}\,d\theta\right|. \qquad (12)$$

In order to demonstrate that Eqs. (1)–(3) can exhibit dynamical behavior associated with the quantum HMF model, we consider two example cases: strong driving, far above threshold, i.e., $p_0 \gg p_{th}$, and weak driving, just above threshold, i.e., p_0 only marginally exceeds p_{th}. These cases of strong
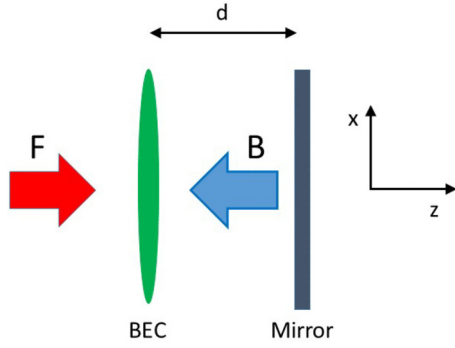
FIG. 1. Schematic diagram of the single mirror feedback (SMF) configuration showing a BEC interacting with a forward propagating optical field (F) and a retroreflected/backward propagating optical field (B).

and weak driving can be interpreted physically as that where the structuring nature of the instability completely dominates delocalizing quantum pressure in the BEC, and that where the effects of quantum pressure are significant, respectively. In both cases we restrict the values of b_0, Δ, etc. such that $\chi_0 n \ll 1$, for consistency with the assumption made when deriving Eq. (11) from Eq. (13). Figure 2 shows an example of self-structuring displayed by the BEC-SMF model, Eqs. (1)–(3), in the case where the system is driven strongly, far above the instability threshold, i.e., $p_0 \gg p_{th}$. The system spontaneously develops a modulated optical intensity and modulated density with a spatial period of Λ_c. The spatio-temporal distribution of the BEC density and optical intensity develop intricate "chevron" structures similar to those observed in Ref. [6] produced by a "quantum Jeans instability" [5].

Figure 3 shows an example of self-structuring when the system is driven weakly, marginally above the instability threshold. Again, both the BEC and optical field spontaneously develop a modulation with a spatial period of Λ_c, but the evolution of the system is qualitatively different from the strongly driven case shown in Fig. 2. In the weakly-driven
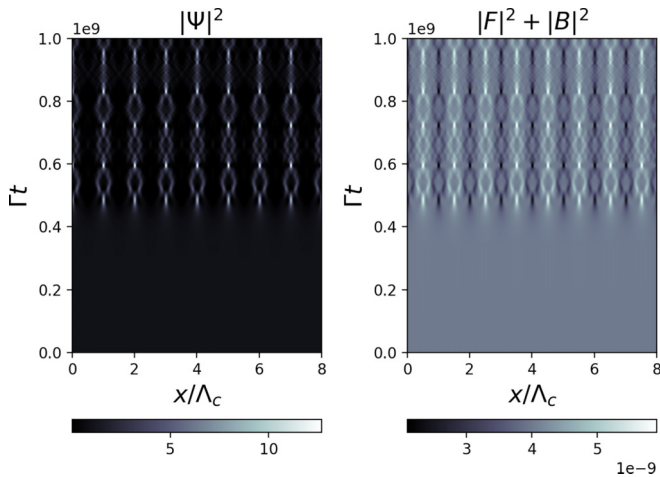

FIG. 2. Evolution of BEC density and optical intensity for strong driving, calculated from Eqs. (1)–(3). Parameters used: $b_0 = 100$, $\Delta = 500$, $p_0 = 10 p_{th} = 2 \times 10^{-9}$, $R = 1$, $\frac{\omega_r}{\Gamma} = 10^{-8}$.
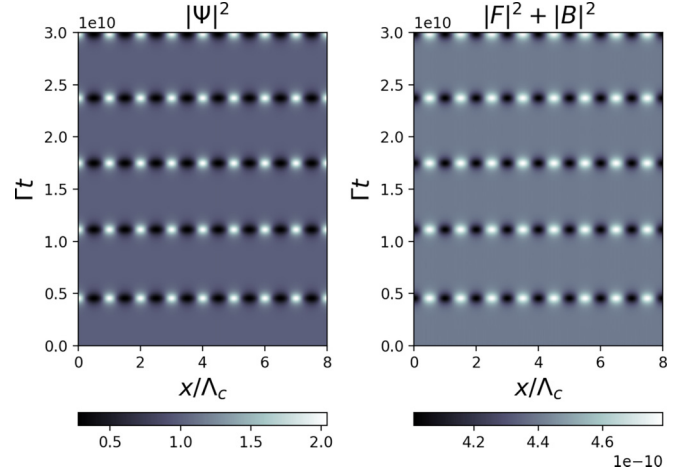

FIG. 3. Evolution of BEC density and optical intensity for weak driving, calculated from Eq. (1)–(3). Parameters used: $b_0 = 100$, $\Delta = 500$, $p_0 = 1.1 p_{th} = 2.2 \times 10^{-10}$, $R = 1$, $\frac{\omega_r}{\Gamma} = 10^{-8}$.

case, the BEC density distribution consists of what were termed "monoclusters" in Ref. [6] and the chevrons are absent. The temporal behavior is also different in the two cases. For weak driving, after development of the optical and BEC structures they disperse and reform regularly whereas in the strongly driven case the temporal behavior is more complex, with a quasiperiodic sequence of dispersal and revival.

This mapping between the BEC-SMF model of Eqs. (1)–(3) and the quantum HMF model when $\chi_0 n \ll 1$ allows us to gain some insight into the behavior of the BEC-SMF system. It explains the similarity in the evolution of the BEC density shown in Fig. 2 with that displayed by the quantum HMF model in Ref. [6], i.e., the chevron structures. In the weakly driven regime, it allows additional insight if we assume a wavefunction of the form

$$\Psi(\theta, t) = c_0(t) + c_1(t)\cos(\theta), \qquad (13)$$

i.e., representing two states, one of which $|0\rangle$ is spatially uniform, and the other $|1\rangle$ which is spatially periodic with spatial period Λ_c. Using this two-state ansatz, the effective GPE equation of the quantum HMF model in Eq. (11) can be rewritten as an equation for the order parameter or "magnetization" M (see Supplementary Material [18]):

$$\left(\frac{dM}{dt}\right)^2 + \frac{\epsilon^2}{2}M^4 - \omega_r^2\left(\frac{\epsilon}{\omega_r} - 1\right)M^2 = 0, \qquad (14)$$

which has the solution

$$M(t) = \sqrt{2}\frac{\omega_r}{\epsilon}\sqrt{\frac{\epsilon}{\omega_r} - 1}\ \text{sech}\left[\omega_r\sqrt{\frac{\epsilon}{\omega_r} - 1}(t - t_0)\right], \qquad (15)$$

where $t_0 = \frac{\cosh^{-1}\left(\frac{\sqrt{2}\frac{\omega_r}{\epsilon}\sqrt{\frac{\epsilon}{\omega_r}-1}}{M_0}\right)}{\omega_r\sqrt{\frac{\epsilon}{\omega_r}-1}}$ and $M_0 = M(t=0)$.

Figure 4 (inset) shows the evolution of M as calculated from Eq. (15) and from the BEC-SMF model [Eqs. (1)–(3)], when the system is driven weakly. The analytical expression for M in Eq. (15) and the numerical calculation agree well for the first period of the evolution, which in the numerical simulation then repeats periodically as in Fig. 3. The behavior
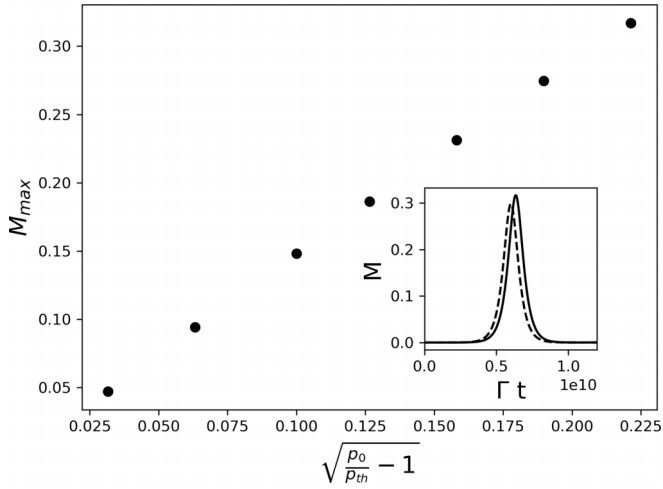
FIG. 4. Maximum value of M as a function of p_0, calculated from Eqs. (1)–(3). All other parameters used are as for Fig. 3. Inset shows evolution of M calculated from Eq. (15) (dashed line), and from a numerical solution of Eqs. (1)–(3) (full line), for one period of oscillation when the system is driven weakly ($p_0 = 1.05$, $p_{th} = 2.098 \times 10^{-10}$). All other parameters used are as for Fig. 3.

of the system in the weakly driven regime is therefore similar to that of a two-state quantum system where the BEC density (and consequently the optical intensity) oscillates spontaneously in time between a spatially uniform state and a spatially structured state. Equation (15) predicts that the maximum value of the order parameter M scales with distance from threshold $\propto (p_0 - p_{th})^{1/2}$, similar to the mean-field Ising model. Figure 4 shows that this scaling behavior is produced by the BEC self-structuring model [Eqs. (1)–(3)].

In addition to formation of global structures, i.e., spatially periodic patterns, it has been shown that spatially lozalized structures can also arise in the BEC-SMF system [17]. These structures were termed "droplets" in Ref. [17] due to the similarity with quantum droplets in dipolar BECs [13,14]. An example of a stable droplet in the BEC-SMF system is shown in Fig. 5 as calculated from Eqs. (1)–(3). It can be seen that a BEC of width smaller than Λ_c maintains its shape due to its interaction with the optical field which it generates. The existence of soliton solutions for the quantum HMF model was discovered in Ref. [7], which showed that they are similar to strongly localized gap solitons which can exist for BECs in optical lattices [19], with the difference that in the quantum HMF model the lattice is not externally imposed, but self-generated by the BEC. Here we show that the mapping of the BEC-SMF system as described by Eqs. (1)–(3) to the quantum HMF model as described by Eq. (11) allows determination of the width of the droplet and its dependence on the parameters of the system, e.g., pump intensity p_0.

Assuming that the profile of the BEC density is Gaussian with width σ_x, i.e., $\Psi(x) \propto \exp(-\frac{x^2}{2\sigma_x^2})$, then the value of σ_x which minimizes the energy functional $E(\sigma_x)$ defined as

$$E(\sigma_x) = \frac{1}{2\pi} \int_0^{2\pi} \Psi^* \left[-\omega_r \frac{\partial^2 \Psi'}{\partial \theta^2} - \epsilon \Phi(x, t) \right] \Psi \, d\theta \quad (16)$$
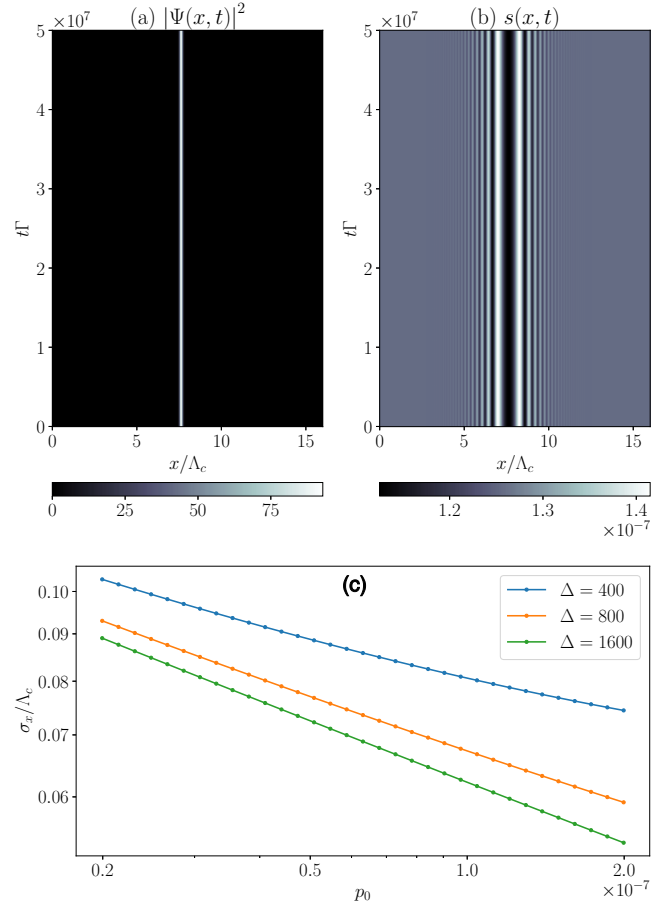

FIG. 5. Evolution of (a) BEC density and (b) optical intensity distribution calculated from Eqs. (1)–(3) showing a stable, localized droplet. The parameters used were $p_0 = 6.3 \times 10^{-8}$, $b_0 = 20$, $\Delta = 1600$, $\omega_r/\Gamma = 1.00 \times 10^{-7}$, and $R = 0.99$. The initial BEC wavefunction was Gaussian with width $\sigma_x/\Lambda_c = 0.07$. (c) Plot (on log-log scale) of stable droplet width σ_x vs pump intensity, p_0 calculated from Eqs. (1)–(3). The parameters used were as for (a) and (b).

can be shown to be (see Supplementary Material [18])

$$\frac{\sigma_x}{\Lambda_c} = \frac{1}{2\pi} \left(\frac{\omega_r}{\epsilon} \right)^{1/4} \propto (p_0 b_0 R)^{-1/4}. \quad (17)$$

This is consistent with a more rigorous derivation of soliton solutions for the quantum HMF model [7], with density profiles described by parabolic cylinder functions of characteristic width $\propto \epsilon^{-1/4}$. The predicted dependence of droplet width σ_x on pump intensity p_0 is confirmed in Fig. 5, where the stable droplet width is calculated from Eqs. (1)–(3) for different pump intensities and is plotted against p_0. The power-law scaling $\sigma_x \propto p_0^{-1/4}$ predicted by energy minimization of the quantum HMF model agrees well with the results of the simulations so long as Δ is sufficiently large that condition $\chi_0 n \ll 1$ is well satisfied. This scaling behavior shows that the profile and characteristic width of these optomechanical droplets are more closely related to those of localized gap solitons [7,19] in a self-generated lattice than to

other types of localized structures, e.g., nonlinear Schrödinger equation solitons or quantum droplets observed in dipolar BECs [13,14].

In conclusion, we have shown that a BEC interacting with an optical field via a feedback mirror can be a realization of the quantum HMF model. We demonstrated that the self-structuring of an initially uniform BEC displays features observed previously in the quantum HMF model: for strong driving, chevrons appear in the BEC density; for weak driving, the BEC behaves as a two-state quantum system, with the order parameter or magnetization evolving as a series of sech pulses. The mapping to the quantum HMF model also allowed predicting the dependence of BEC droplet width on pump intensity, which agreed well with simulations of the BEC-SMF model. These results suggest that optical diffraction-mediated interaction between atoms in a BEC may be a promising candidate for experimental realization of quantum HMF dynamics and consequently be a versatile testing ground for models of quantum systems involving long-range interactions.

[1] T. Dauxois *et al.* (eds.), *Long-Range Interacting Systems*, Lecture Notes in Physics, Vol. 602 (Springer-Verlag, Berlin, Heidelberg, 2002), pp. 458–487.

[2] N. Defenu, T. Donner, T. Macrì, G. Pagano, S. Ruffo, and A. Trombettoni, Long-range interacting quantum systems, arXiv:2109.01063.

[3] P. Chavanis, J. Vatteville, and F. Bouchet, Dynamics and thermodynamics of a simple model similar to self-gravitating systems: the HMF model, Eur. Phys. J. B **46**, 61 (2005).

[4] P.-H. Chavanis, The quantum HMF model: I. Fermions, J. Stat. Mech. (2011) P08002.

[5] P.-H. Chavanis, The quantum HMF model: II. Bosons, J. Stat. Mech. (2011) P08003.

[6] R. Plestid, P. Mahon, and D. H. J. O'Dell, Violent relaxation in quantum fluids with long-range interactions, Phys. Rev. E **98**, 012112 (2018).

[7] R. Plestid, and D. H. J. O'Dell, Balancing long-range interactions and quantum pressure, Phys. Rev. E **100**, 022216 (2019).

[8] G. R. M. Robb, N. Piovella, A. Ferraro, R. Bonifacio, Ph. W. Courteille, and C. Zimmermann, Collective atomic recoil lasing including friction and diffusion effects, Phys. Rev. A **69**, 041403(R) (2004).

[9] C. von Cube, S. Slama, D. Kruse, C. Zimmermann, Ph. W. Courteille, G. R. M. Robb, N. Piovella, and R. Bonifacio, Self-Synchronization and Dissipation-Induced Threshold in Collective Atomic Recoil Lasing, Phys. Rev. Lett. **93**, 083601 (2004).

[10] R. Bachelard, T. Manos, P. de Buyl, F. Staniscia, F. S. Cataliotti, G. De Ninno, D. Fanelli, and N. Piovella, Experimental perspectives for systems based on long-range interactions, J. Stat. Mech. (2010) P06009.

[11] S. Schütz and G. Morigi, Prethermalization of Atoms Due to Photon-Mediated Long-Range Interactions, Phys. Rev. Lett. **113**, 203002 (2014).

[12] K. Baumann, C. Guerlin, F. Brennecke and T. Esslinger, Dicke quantum phase transition with a superfluid gas in an optical cavity, Nature (London) **464**, 1301 (2010).

[13] I. Ferrier-Barbut, H. Kadau, M. Schmitt, M. Wenzel, and T. Pfau, Observation of Quantum Droplets in a Strongly Dipolar Bose Gas, Phys. Rev. Lett. **116**, 215301 (2016).

[14] L. Chomaz, S. Baier, D. Petter, M. J. Mark, F. Wächtler, L. Santos, and F. Ferlaino, Quantum-Fluctuation-Driven Crossover from a Dilute Bose-Einstein Condensate to a Macro-droplet in a Dipolar Quantum Fluid, Phys. Rev. X **6**, 041039 (2016).

[15] G. R. M. Robb, E. Tesio, G.-L. Oppo, W. J. Firth, T. Ackemann, and R. Bonifacio, Quantum Threshold for Optomechanical Self-Structuring in a Bose-Einstein Condensate, Phys. Rev. Lett. **114**, 173903 (2015).

[16] G. Labeyrie, E. Tesio, P. M. Gomes, G. L. Oppo, W. J. Firth, G. R. M. Robb, A. S. Arnold, R. Kaiser and T. Ackemann, Optomechanical self-structuring in a cold atomic gas, Nat. Phot. **8**, 321 (2014).

[17] Y.-C. Zhang, V. Walther, and T. Pohl, Long-Range Interactions and Symmetry Breaking in Quantum Gases through Optical Feedback, Phys. Rev. Lett. **121**, 073604 (2018).

[18] See Supplemental Material at http://link.aps.org/supplemental/10.1103/PhysRevResearch.5.L032004 for derivations of the magnetization evolution and stable droplet width together with the conditions required for neglect of incoherent scattering during self-structuring.

[19] P. J. Y. Louis, E. A. Ostrovskaya, C. M. Savage, and Y. S. Kivshar, Bose-Einstein condensates in optical lattices: Band-gap structure and solitons, Phys. Rev. A **67**, 013602 (2003).